SO-3, a new O-superfamily conopeptide derived from *Conus striatus*, selectively inhibits N-type calcium currents in cultured hippocampal neurons

[1]Lei Wen, [1]Sheng Yang, [1]Haifa Qiao, [1]Zhenwei Liu, [1]Wenxia Zhou, *,[1]Yongxiang Zhang & [2]Peitang Huang

[1]Beijing Institute of Pharmacology and Toxicology, 27 Tai-Ping Road, Haidian District, Beijing 100850, China and [2]Beijing Institute of Biotechnology, Beijing, China

1 Whole-cell currents in cultured hippocampal neurons were recorded to investigate the effects of SO-3, a new O-superfamily conopeptide derived from *Conus striatus*, on voltage-sensitive channels.

2 SO-3 had no effect on voltage-sensitive sodium currents, delayed rectifier potassium currents, and transient outward potassium currents.

3 Similar to the selective N-type calcium channel blocker ω-conotoxin MVIIA (MVIIA), SO-3 could concentration-dependently inhibit the high voltage-activated (HVA) calcium currents (I_{Ca}).

4 MVIIA(3 μM), 10 μM nimodipine, and 0.5 μM ω-agatoxin IVA (Aga) could selectively block the N-, L-, and P/Q-type I_{Ca}, which contributed $\sim$32, $\sim$38, and $\sim$21% of the HVA currents in hippocampal neurons, respectively. About 31% of the total HVA currents were inhibited by 3 μM SO-3. SO-3 (3 μM) and 3 μM MVIIA inhibited the overlapping components of HVA currents, whereas no overlapping component was inhibited by 3 μM SO-3 and 10 μM nimodipine, or by 3 μM SO-3 and 0.5 μM Aga. Also, 3 μM SO-3 had no effect on R-type currents.

5 SO-3 had less inhibitory effects on non-N-type HVA currents than MVIIA at higher concentrations (30 and 100 μM).

6 The inhibitory effects of SO-3 and MVIIA on HVA currents were almost fully reversible. However, the recovery from block by MVIIA was more rapid than recovery from block by SO-3.

7 It is concluded that SO-3 is a new ω-conotoxin selectively targeting N-type voltage-sensitive calcium channels. Considering the significance of N-type calcium channels for pain transduction, SO-3 may have therapeutic potential as a novel analgesic agent.
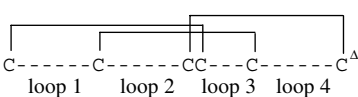
Introduction

Conopeptides are small, structured peptide toxins secreted by the venomous marine snails of the genus *Conus* for prey capture, defense, and competitor deterrence. It is now clear that in the venoms of living species in the genus *Conus* there are about 50,000 different conotoxins, most of which are 12–30 amino acids in length and contain two to four disulfide bridges, and can selectively target a specific voltage-gated ion channel, ligand-gated ion channel, or G-protein-coupled receptor. These potential pharmaceutical benefits have led to the use of certain conotoxins as tools for ion channel research as well as for the treatment and diagnosis of neurological diseases (Nielsen *et al.*, 2000; Olivera & Cruz, 2001; Terlau & Olivera, 2004).

Conotoxins are defined to a number of structural classes according to the characteristic arrangement of Cys-residues. The O-superfamily, which contains four-loop, 6-Cys peptides, comprises ω-conotoxins (voltage-sensitive calcium channel (VSCC) blockers), κ-conotoxins (voltage-sensitive potassium channel (VSPC) blockers), μO-conotoxins (voltage-sensitive sodium channel (VSSC) blockers), and δ-conotoxins (inhibitors of the fast inactivation of VSSCs). These four classes of conotoxins are unusually hydrophobic peptides with the same cysteine framework C–C–CC–C–C, giving these peptides a similar inhibitory cysteine knot (ICK) motif (Table 1) (Nielsen *et al.*, 2000; Olivera & Cruz, 2001; Terlau & Olivera, 2004).

The individual peptides in one conotoxin family may selectively target a diverse set of different molecular isoforms within the same ion channel family. For example, ω-conotoxin

*Author for correspondence; E-mail: zhangyx@nic.bmi.ac.cn

Table 1 Selected O-superfamily conopeptides targeting different voltage-sensitive ion channels

Peptide	Conus *Specie*	Sequence[a]	Targeted ion channel[b]	Reference
		C------C------CC---C------C△		
		loop 1 loop 2 loop 3 loop 4		
ω-GVIA	*C. geographus*	CKSOGSSCSOTSYNCCR-SCNOYTKRCY* (4)	VSCCs, N-type	Olivera *et al.* (1984)
ω-MVIIA	*C. magus*	CKGKGAKCSRLMYDCCTGSC-RSGKC* (5)	VSCCs, N-type	Olivera & Cruz (2001)
ω-MVIIC	*C. magus*	CKGKGAPCRKTMYDCCSGSCGRR-GKC* (6)	VSCCs, P/Q/N-type	Hillyard *et al.* (1992)
ω-CVIA	*C. catus*	CKSTGASCRRTSYDCCTGSC-RSGRC* (4)	VSCCs, N-type	Lewis *et al.* (2000)
ω-CVIB	*C. catus*	CKGKGASCRKTMYDCCRGSC-RSGRC* (6)	VSCCs, N/P/Q-type	Lewis *et al.* (2000)
ω-CVIC	*C. catus*	CKGKGQSCSKLMYDCCTGSCSRR-GKC* (5)	VSCCs, N/P/Q-type	Lewis *et al.* (2000)
ω-CVID	*C. catus*	CKSKGAKCSKLMYDCCSGSCSGTVGRC* (4)	VSCCs, N-type	Lewis *et al.* (2000)
ω-SVIA	*C. striatus*	CRSSGSPCGVTS-ICC-GRC-YRGKCT* (4)	poor activity on VSCCs	Ramilo *et al.* (1992)
ω-SVIB	*C. striatus*	CKLKGQSCRKTSYDCCSGSCG-RSGKC* (5)	VSCCs, P/Q-type	Ramilo *et al.* (1992)
SO-3[c]	*C. striatus*	CKAAGKPCSRIAYNCCTGSC-RSGKC* (5)	?	
δ-SVIE	*C. striatus*	DGCSSGGTFCGIHOGLCCSEFCFLWCITFID	VSSCs	Bulaj *et al.* (2001)
μO-MrVIA	*C. marmoreus*	ACRKKWEYCIVPIIGFIYCCPGLICGPFVCV	VSSCs	McIntosh *et al.* (1995)
μO-MrVIB	*C. marmoreus*	ACSKKWEYCIVPILGFVYCCPGLICGPFVCV	VSSCs	McIntosh *et al.* (1995)
κ-PVIIA	*C. purpurascens*	CRIONQKCFQHLDDCCSRKCNRFNKCV	VSPCs	Shon *et al.* (1998)

[a]All ω-conotoxins are C-terminally amidated (*), each net positive charge is indicated in the braces after the sequence of the corresponding ω-conotoxin. The disulfide bridges motif of ω-conotoxins and its four loops (△) are also displayed above the sequences.
[b]Targeted ion channels are determined from radioligand binding and/or electrophysiology experiments.
[c]GenBank accession number of the SO-3 cDNA sequence is AF46350.

MVIIA and MVIIC, both derived from *Conus magus*, have high identity in sequence, but quite different selectivity: MVIIA is highly selective for N-type VSCCs, whereas MVIIC is more selective for the P/Q-type (Nielsen *et al.*, 1999a). Among the ω-conotoxins CVIA–CVID, all identified from *C. catus*, CVIA and CVID are selective towards the N-type VSCCs, while CVIB and CVIC show no difference between N- and P/Q-type VSCCs (Lewis *et al.*, 2000; Nielsen *et al.*, 2000; Adams *et al.*, 2003). On the other hand, peptides derived from different cone snail species, although their conopeptide sequences vary largely except the cysteine framework, may act on the same ion channel subtype, as both ω-conotoxin MVIIA and GVIA can block the same N-type VSCCs (Olivera & Cruz, 2001; Terlau & Olivera, 2004) (Table 1).

The venoms of each species always contain a unique array of more than 100 peptides, which are used by the genus *Conus* for divergent biotic purposes. For this reason, corresponding venom components with divergent pharmacological properties in one particular *Conus* species are expected. In searching for new conotoxins with some therapeutic potential, more than 25 species of *Conus* from the South China Sea have been collected. Also, by gene screening, we identified a new conopeptide termed SO-3 from a fish-eating snail, *C. striatus* (Lu *et al.*, 1999). SO-3 contains 25 amino-acid residues and the same cysteine framework as O-superfamily conotoxins. Previously, three O-superfamily conopeptides, including two ω-conotoxins (SVIA and SVIB) and one δ-conotoxin (SVIE), have been isolated from the venom of *C. striatus* biochemically (Table 1) (Ramilo *et al.*, 1992; Bulaj *et al.*, 2001). SO-3 shows 56% sequence identity with SVIB, a P/Q-type VSCCs blocker, and 72% with MVIIA, an N-type VSCC blocker. In addition, it has the same positive charges as SVIB and MVIIA (Table 1). Further bioactivity evaluation on the synthetic SO-3 showed that SO-3 is a potent analgesic agent with effects similar to MVIIA (Dai *et al.*, 2003). However, the ion channel target of SO-3 is still unclear. Here, we observed the effects of SO-3 on voltage-sensitive ion currents in primary cultured hippocampal neurons. The results indicated that SO-3 is a selective N-type VSCC blocker.

Methods

Cell culture

Primary cultures of hippocampal cells were established using a modification of the previous procedure (Banker & Cowan, 1979). Wistar rats at postnatal day 1 were deeply anesthetized with ether and decapitated, in accordance with the guideline of the Beijing Institutes for Biological Sciences Animal Research Advisory Committee. The hippocampi were dissected in ice-cold Ca^{2+}- and Mg^{2+}-free PBS, incubated at 37°C with 0.125% trypsin (type XI; Sigma Co., Ltd, St Louis, MO, U.S.A.) for 20 min, and then triturated to dissociate cells. After being washed, the single cell suspension was diluted with Dulbecco's modified Eagle's medium (DMEM) supplemented with 10% fetal bovine serum (FBS), 10% horse serum (HS), 100 U ml^{-1} penicillin, and 100 μg ml^{-1} streptomycin. Cells were plated in 35 mm plastic culture dishes (Nunc, Denmark) pre-coated with poly-L-lysine (75 μg ml^{-1}) at a density of 5.0×10^5 cells per dish, and cultured at 37°C in a humidified atmosphere containing 5% CO_2 and 95% air. After 24-h incubation, the culture medium was changed to 2 ml of DMEM containing 10% FBS, 2 mM glutamine, 1% N_2, 100 U ml^{-1} penicillin, and 100 μg ml^{-1} streptomycin. The proliferation of non-neuronal cells was controlled by treating with 3 μM cytosine arabinofuranoside (c-Ara) for 48 h at the second day in culture. Subsequently, half of the medium was replaced twice a week. All experiments were performed on cells aging 10–12 days *in vitro*. c-Ara was purchased from Sigma Co., Ltd, and other reagents including DMEM, FBS, HS, and N_2 were obtained from GIBCO Life Technologies (Rockville, MD, U.S.A.).

Recording solutions

The extracellular solution for whole-cell recordings contained (in mM): NaCl 140, KCl 5, $MgCl_2$ 1, $CaCl_2$ 2, Dextrose 10,

HEPES 10. The pH for extracellular solution was adjusted to 7.4 with NaOH and the osmolarity was adjusted to 320 mOsm with sucrose. For K^+ current recording, the extracellular solution was supplemented with 1 μM tetrodotoxin (TTX) to block Na^+ channels, and 0.4 mM $CdCl_2$ to block all Ca^{2+} channels and Ca^{2+}-activated K^+ channels. For Na^+ current recording, the same extracellular solution was used, except TTX was replaced with 5 mM tetraethylammonium chloride (TEA-Cl) and 2 mM 4-aminopyridine (4-AP) to block the delayed rectified K^+ channels and transient outward K^+ channels, respectively, For Ca^{2+} current recording, 1 μM TTX, 5 mM TEA-Cl, and 2 mM 4-AP were added to the extracellular solution to block Na^+ channels and K^+ channels. The intracellular pipette solution used for K^+ current recording contained (in mM): KCl 140, HEPES 10, EGTA 10, and ATP-Na_2 2, and the pH was adjusted to 7.2 by KOH. For Na^+ and Ca^{2+} current recording, the solution contained (in mM): CsCl 140, HEPES 10, EGTA 10, TEA-Cl 5, and ATP-Na_2 2, and the pH was adjusted to 7.2 by CsOH. The osmolarity of the pipette solutions was adjusted to 320 mOsm. TEA-Cl, 4-AP, TTX, $CdCl_2$, and ATP-Na_2 were purchased from Sigma Co., Ltd.

Electrophysiology recordings

Patch pipettes (with resistances of 2–4 MΩ after being filled with intracellular solutions) were prepared using a two-stage microelectrode puller (PC-10; Narishige, Tokyo, Japan) and fire-polished using a MF-830 microforge (Narishige) just before recording. All experiments were carried out under room temperature (20–22°C). Voltage-clamp recordings were performed in the whole-cell patch-clamp configuration according to standard patch-clamp methods (Hamill *et al.*, 1981) using an Axopatch 200B patch-clamp amplifier (Axon Instruments, Foster City, CA, U.S.A.). Data were sampled at 5 kHz and filtered at 2 kHz (−3 dB, four-pole Bessel filter) on-line by using the pCLAMP 8.2 software (Axon Instruments, Foster City, CA, U.S.A.). Series resistance was compensated (>80%) in all experiments, and leak subtraction was carried out using a P/−4 protocol online. For all experiments, as soon as the whole-cell configuration had been acquired, current was allowed to stabilize for approximately 5 min before the experimental voltage command was administered. Only those recordings with stable holding currents and access resistance were accepted. Cells showing current rundown at a rate of currents more than 1% min^{-1} in the absence of treatments were discarded. All calcium currents (I_{Ca}) were normalized for differences in cell sizes by transformation to current density (pA pF^{-1}; dividing each current (I_{ca}) measure by the whole-cell membrane capacitance for that cell).

Drugs and drug application

The synthesis, folding, and purification of SO-3 were performed in Beijing Institute of Biotechnology, China as described in Dai *et al.* (2003). Using the designated conditions, the folding peptide of SO-3 was obtained in greater than 98% purity after two steps of HPLC purification. The final peptide content in lyophilized powder was approximately 79%. Using MALDI-TOF, the molecular mass (single isotope) of SO-3 was 2560.1 Da, in agreement with the calculated molecular mass of 2561.1 Da. Nimodipine, ω-conotoxin MVIIA (MVIIA), and ω-agatoxin IVA (Aga) were purchased from Sigma Co., Ltd.

Nimodipine was stored in opaque containers at −20°C as a 10 mM stock solution in 100% ethanol. SO-3, MVIIA, and Aga were dissolved in extracelllular solutions to make 1 mM stock solutions that were aliquot and stored at −20°C. Each stock solution was diluted to the test concentration with extracelular solution. Bovine serum albumin (BSA (1 mg ml^{-1}); Sigma) was present in all final extracelular solutions to prevent the nonspecific binding of peptides. To control for vehicle effects, 0.1% (v v^{-1}) ethanol was present in the extracelular solutions throughout the experiments when nimodipine would be applied, and experiments were performed under restricted light conditions. During the experiments, cells were rinsed twice with extracellular solution, then continuously perfused with the test concentration of drug(s) by using a gravity-fed bath perfusion system. The flow rate was approximately 5 × 10^{-3} ml s^{-1}. The distance of the flow pipette from the cell was approximately 150 μm and the pipette tip diameter was about 300 μm. The total volume of the extracellular solution was kept in 1.5 ml during the experiments.

Data analysis

The concentration–response curves for the effects of SO-3 and MVIIA on the high voltage-activated (HVA) I_{Ca} were fitted according to the logistic equation

$$E(C)/E_{max} = 1/[1 + (C/EC_{50})^{n_H}]$$

where C is the concentration of SO-3 or MVIIA, $E(C)$ is the effect evoked by SO-3 or MVIIA at concentration C, E_{max} denotes the maximal possible effect, EC_{50} is the concentration at which half-maximal effect is obtained. n_H is the Hill coefficient. Origin 6.0 (OriginLab, Northampton, MA, U.S.A.) software was used to perform nonlinear fit of data. SPSS 12.0 software (SPSS Inc., Chicago, IL, U.S.A.) was used for statistical analysis. All data are expressed as mean ± s.e.m., and $P < 0.05$ indicates statistically significant.

Results

No effect of SO-3 on voltage-sensitive sodium currents (I_{Na})

Hippocampal neurons were clamped at a holding potential (V_h) of −80 mV, and depolarized to −40 mV at 10 s intervals to activate inward Na^+ currents which were blocked by 1 μM TTX completely and reversibly (data were not shown). After a 3-min application of 1, 10, and even 100 μM SO-3, the I_{Na} amplitudes were not affected. The current–voltage (I–V) curves remained unaffected after application of 100 μM SO-3. These observations indicated that SO-3 had no effect on I_{Na} (Figure 1).

No effect of SO-3 on delayed rectifier potassium currents ($I_{K(DR)}$) and transient outward potassium currents ($I_{K(A)}$)

$I_{K(DR)}$ and $I_{K(A)}$ were isolated using the electrophysiological and pharmacological methods (Yang *et al.*, 2001). The experimental pulse protocols and subtraction procedure are shown in Figure 2a. Currents at the end of the depolarizing pulse (148 ms) were referred to as $I_{K(DR)}$. The peak currents of
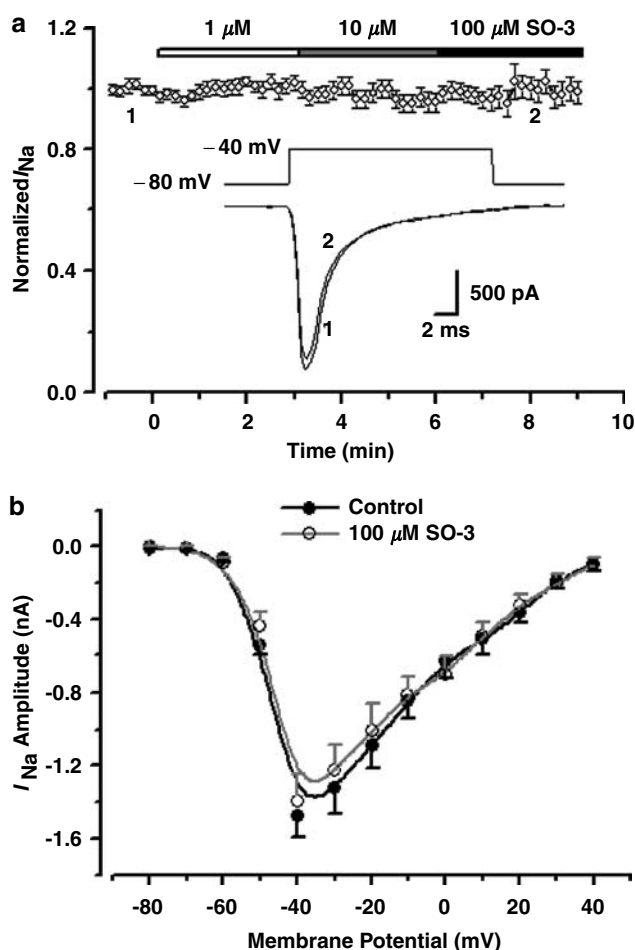
Figure 1 No effect of SO-3 on voltage-sensitive I_{Na} in primary cultured hippocampal neurons. (a) The time course of the effects of 1, 10 and 100 μM SO-3 on peak I_{Na}. Currents were evoked by 20 ms depolarizing voltage step commands from a V_h of -80 to -40 mV at 10 s intervals. Peak I_{Na} amplitudes were normalized to the values in the absence of SO-3 and plotted against exposure time. Data are shown as mean$\pm$s.e.m., $n=13$. Drugs were applied to the cell as indicated by the horizontal bar. Inset: Pulse paradigm and the representative current traces at the time point 1 (black) and 2 (gray). (b) *I–V* relationship of peak I_{Na} before and after 2-min exposure to 100 μM SO-3. Each point represents the mean of eight cells. I_{Na}'s were evoked by a series of 20 ms depolarizing steps from a V_h of -80 to $+40$ mV, with 10 mV increments and 2 s intervals.

the subtracted traces were referred to as $I_{K(A)}$. As Figure 2b and c showed, no significant effect on $I_{K(DR)}$ and $I_{K(A)}$ was observed after exposure to 100 μM SO-3.

Concentration-dependent inhibition of SO-3 on HVA I_{Ca}

HVA I_{Ca} were evoked by 150 ms depolarizing voltage step commands from a V_h of -80 mV in primary cultured hippocampal neurons. Under the present experiments procedure, the inward I_{Ca} reached maximum amplitude when depolarizing to 0 mV. Figure 3 indicated a concentration-dependent inhibition of SO-3 on HVA I_{Ca}, and these inhibitory effects were similar to that of MVIIA, a determined N-type calcium channel blocker. In most cases, the inhibitory effects of a given concentration of peptides occurred within 10–20 s application and reached a stable maximum after 30–50 s. For

both SO-3 and MVIIA, there was a plateau of inhibition at 1–3 μM. The calculated EC_{50}'s for SO-3 and MVIIA were 0.16 and 0.20 μM, respectively.

Inhibitory effects of SO-3 on I–V relationships of I_{Ca}

To identify whether the inhibition of I_{Ca} caused by SO-3 in cultured hippocampal neurons is voltage-dependent, the *I–V* relationships in the presence or absence of SO-3 were studied (Figure 4). These results confirmed the concentration-dependent inhibition on I_{Ca} after 2-min exposure to 0.03, 0.3, and 3 μM SO-3. The inhibitory effects of SO-3 on I_{Ca} were obvious at the potentials between -20 and $+40$ mV, and no obvious I_{Ca} was inhibited below the potential of -30 mV. These results indicated that SO-3 had inhibitory effects on HVA I_{Ca}, other than on low voltage-activated (LVA), that is, T-type currents. *I–V* relationships also showed no significant change of the threshold of activation of I_{Ca} and the reversal potential after application of SO-3. In order to illustrate the effects of SO-3 more clearly, the *I–V* curve of the 3 μM SO-3-sensitive currents was obtained by subtracting the currents in the presence of 3 μM SO-3 from the currents in the absence of 3 μM SO-3. The *I–V* curve of the subtracted 3 μM SO-3-sensitive currents was very similar to the subtracted 3 μM MVIIA-sensitive currents, indicated that, at the concentration of 3 μM, SO-3 and MVIIA had similar effects on *I–V* relationships of I_{Ca}.

Selectivity of SO-3 on VSCC subtype

Previous experiments have proved the inhibitory effects of SO-3 on HVA I_{Ca}; here, we further examined whether HVA I_{Ca} inhibited by SO-3 is VSCC-subtype selective. At least four distinct types of HVA VSCCs (L-, N-,P/Q-, and R-type) are expressed in cultured hippocampal neurons and sensitive to different blockers (Currie & Fox, 1997; Nakashima *et al.*, 1998; Newcomb *et al.*, 1998; Blalock *et al.*, 1999; Scamps *et al.*, 2000). In our studies, SO-3 and one of three distinct VSCC blockers (MVIIA, nimodipine or Aga) were additionally applied to cultured hippocampal neurons in three separate experiments with drug presentation order reversed (Figures 5–7). According to previous reports (Nakashima *et al.*, 1998; Blalock *et al.*, 1999; Scamps *et al.*, 2000), 10 μM nimodipine, 3 μM MVIIA, and 0.5 μM Aga were used to define L-, N-, and P/Q-type currents in these experiments, respectively. SO-3 (3 μM) was also used. Typically, SO-3, MVIIA, and Aga required 30–50 s exposure to give stable inhibition, whereas nimodipine acted more rapidly ($\sim$20–30 s).

As Figure 5 showed, after application of 3 μM SO-3 or MVIIA, the inhibition amounts of HVA I_{Ca} were similar ($\sim$31 and $\sim$32%, respectively), and no further inhibition was observed after additional application of the other drug. The remained HVA I_{Ca} could be blocked almost completely by 0.4 mM $CdCl_2$ within 20 s (data were not shown). These results suggested that SO-3 and MVIIA inhibited the overlapping components of HVA I_{Ca} in cultured hippocampal neurons (two-way ANOVA on repeated measures, $P<0.001$ for presentation order), and there was no significant difference between the effects of SO-3 and MVIIA ($P=0.872$ for drug type). Therefore, these two drugs may share a common site of inhibition in this preparation. Unlike the experiments described above, sequential addition of SO-3 and nimodipine, and SO-3 and Aga, both produced additive inhibition on HVA
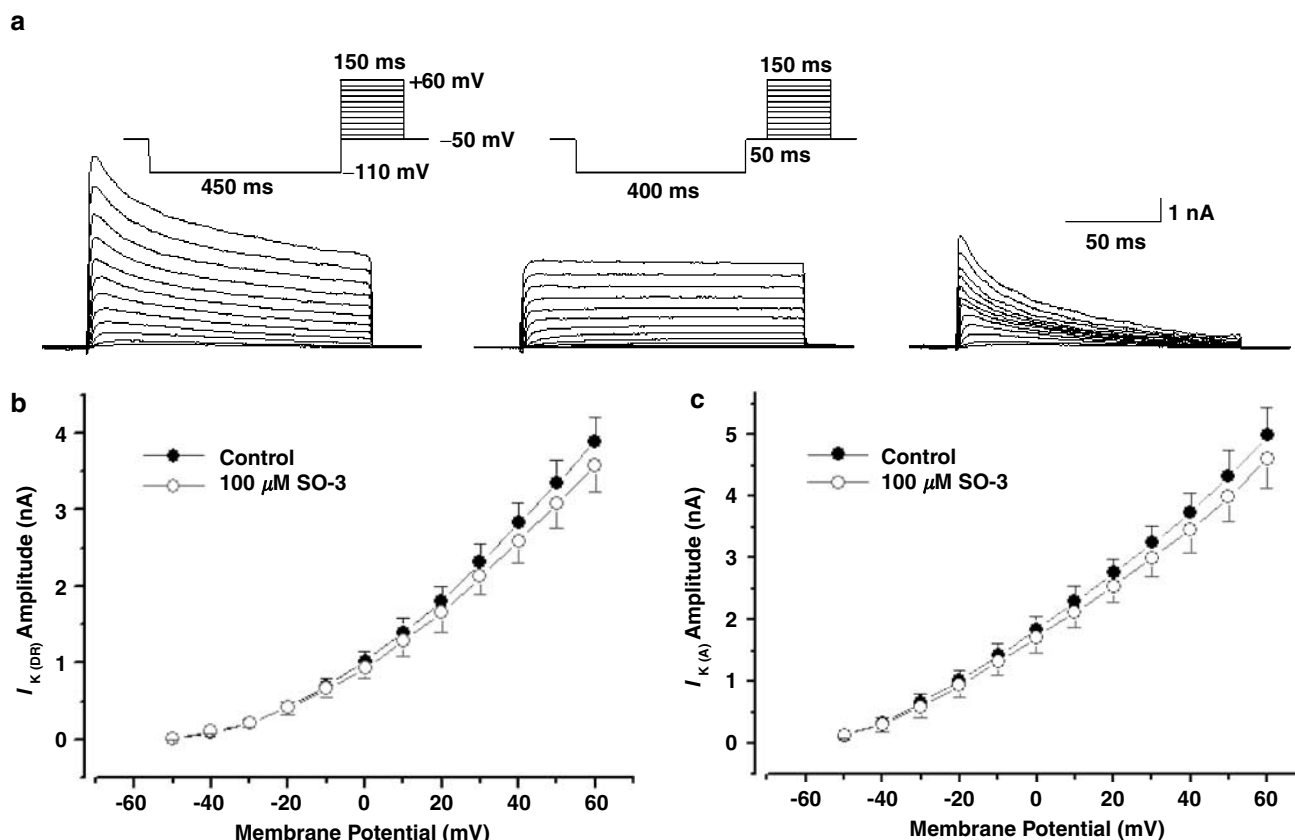
a

b

c

Figure 2 No effect of SO-3 on voltage-sensitive potassium currents. (a) The example family traces of outward potassium currents (I_K) (left), $I_{K(DR)}$ (middle) and $I_{K(A)}$ (right). The upper inset shows the stimulus waveforms of I_K and $I_{K(DR)}$, respectively. I_K were evoked by 150 ms depolarizing pulses from -50 to $+60$ mV in 10 mV steps following a hyperpolarizing prepulse of 450 ms to -110 mV. $I_{K(DR)}$ were elicited using a similar protocol, except that for a 50 ms interval at -50 mV was inserted after the hyperpolarizing prepulse of 400 ms to -110 mV. $I_{K(A)}$ were isolated by subtracting the trace of $I_{K(DR)}$ from I_K. (b, c) I–V curves of $I_{K(DR)}$ and $I_{K(A)}$, both $n = 9$. Currents were recorded before (black) and after (gray) 2-min exposure to 100 μM SO-3.

I_{Ca}; 3 μM SO-3-, 10 μM nimodipine-, and 0.5 μM Aga-sensitive currents contributed ~ 31, ~ 38, and $\sim 21\%$ of the total HVA I_{Ca}, respectively, regardless of the presentation order of these blockers (for the presentation order, for SO-3/nimodipine pair, $P = 0.682$; for SO-3/Aga pair, $P = 0.544$), and there were significant differences between the effects of SO-3 and nimodipine ($P = 0.008$), and between SO-3 and Aga ($P = 0.001$) (Figures 6 and 7). These results indicated that no overlapping component of HVA I_{Ca} was inhibited by SO-3 and nimodipine, or by SO-3 and Aga, and suggested that SO-3 did not inhibit L- and P/Q-type currents at the concentration tested.

The effects of SO-3 on R-type HVA I_{Ca} were further examined. L-, N-, and P/Q-type currents were blocked by 10 μM nimodipine, 3 μM MVIIA, and 0.5 μM Aga, and the isolated R-type currents contributed $\sim 12\%$ of the total HVA I_{Ca}. After exposure to 3 μM SO-3, the R-type currents remained unaffected (Figure 8). These results also suggested that SO-3 did not inhibit R-type currents at the concentration tested.

Several previous studies have demonstrated that ω-conotoxin GVIA and MVIIA can block the heterologously expressed L-, P/Q-, and R-type VSCCs at high concentrations (Williams *et al.*, 1992b; Zhang *et al.*, 1993; Feng *et al.*, 2003). We also observed the effects of the higher concentrations of

SO-3 on non-N-type HVA I_{Ca} in cultured hippocampal neurons. As Figure 9 showed, 3 μM SO-3 and MVIIA were first applied to block the N-type I_{Ca}, the remaining HVA I_{Ca}'s were both further inhibited by additional application of 30 and 100 μM SO-3 and MVIIA. About 7 and 13\% of the total HVA I_{Ca} were further inhibited by 30 and 100 μM SO-3, respectively, and more fractions of HVA I_{Ca} (~ 15 and $\sim 37\%$, respectively) were further inhibited by 30 and 100 μM of MVIIA (unpaired Student's *t*-test, $P < 0.01$). These results indicated that SO-3 had less inhibitory effects on non-N-type VSCCs than MVIIA at high concentrations.

Reversibility of the inhibitory effects of SO-3 on HVA I_{Ca}

The different degree of recovery from the block effects of several ω-conotoxins, including GVIA, MVIIA, and CVID, on VSCCs was reported previously (Williams *et al.*, 1992a; Kristipati *et al.*, 1994; Lin *et al.*, 1997; Stocker *et al.*, 1997; Feng *et al.*, 2001; 2003; Liang & Elmslie, 2002; Mould *et al.*, 2004). Under the present experiments procedure, the inhibitory effects of SO-3 and MVIIA on HVA I_{Ca} were both almost fully reversible. However, the recovery from block by MVIIA was more rapid than recovery from block by SO-3. The half-time for recovery for SO-3 and MVIIA were 7.52 ± 0.56 min
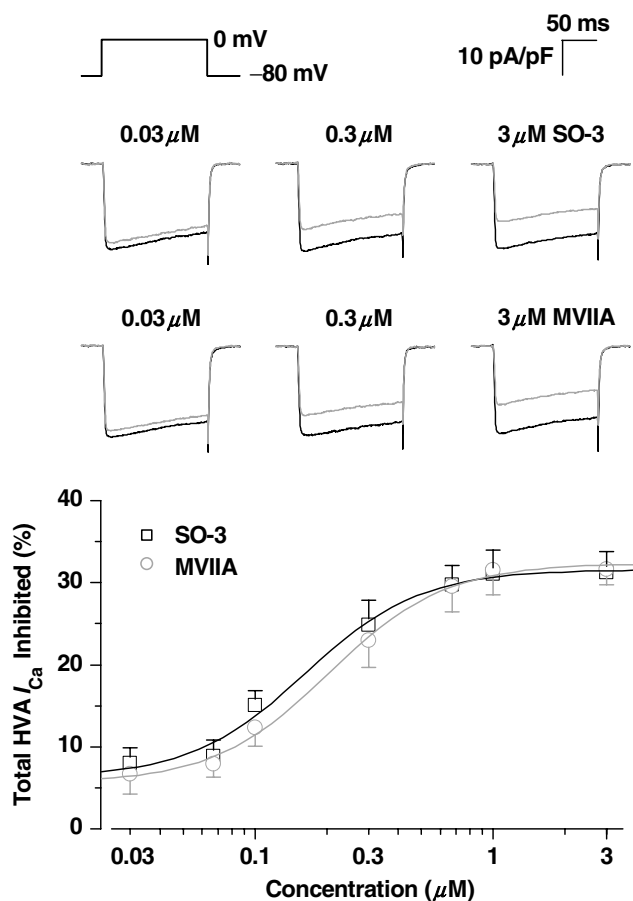
Figure 3 Concentration-dependent inhibition of SO-3 on HVA I_{Ca}. Currents were evoked by depolarizing step pulse from -80 to $0\,mV$ with $150\,ms$ duration. Upper: The representative current traces before (black) and after (gray) 2-min exposure to 0.03, 0.3, and $3\,\mu M$ SO-3 or MVIIA. Lower: Semilog concentration–response curves for the percentage inhibition of peak HVA I_{Ca} by SO-3 or MVIIA, which were fitted with the logistic equation $E(C)/E_{max} = 1/[1 + (C/EC_{50})^{n_H}]$ (see Methods). Data are shown as mean$\pm$s.e.m. For SO-3 groups $n=6$–15, and for MVIIA $n=5$–8. There is no significant difference of the inhibition rates between SO-3 and MVIIA under each concentration (unpaired Student's two-tailed t-test, $P>0.05$).The EC_{50}, E_{max} and n_H values for SO-3 were $0.16\,\mu M$, 31.58% and 1.80, respectively; for MVIIA, they were $0.20\,\mu M$, 32.37% and 1.78, respectively.

and $4.14\pm0.45\,min$, respectively (unpaired Student's t-test, $P<0.01$) (Figure 10).

Discussion

Voltage-sensitive ion channel currents were well characterized to date in primary cultured hippocampal neurons, which gives facilities for the identification of the distinct ion channel target of SO-3. The main finding in this study is that SO-3, a new conopeptide which has the same disulfide bond motif as the O-superfamily conotoxins, selectively inhibits N-type voltage-sensitive I_{Ca} and has no effect on voltage-sensitive sodium and potassium currents.

Ion channels target of SO-3

In our experiments, I_{Na}, $I_{K(DR)}$, $I_{K(A)}$ and I_{Ca}, in primary cultured hippocampal neurons were isolated using the electro-
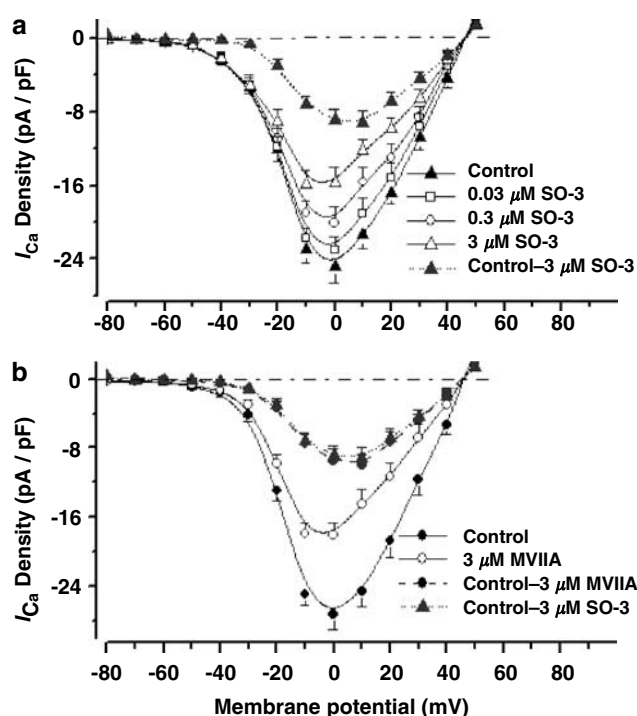

Figure 4 Inhibitory effects of SO-3 on I–V relationship of I_{Ca}. I_{Ca} were evoked by $150\,ms$ depolarizing step commands from -80 to $+50\,mV$ with $10\,mV$ increments and $10\,s$ intervals. (a) I–V curves of peak I_{Ca} density before (Control) and after 2-min exposure to 0.03, 0.3, and $3\,\mu M$ SO-3; the I–V curve of $3\,\mu M$ SO-3-sensitive current density (Control $- 3\,\mu M$ SO-3, obtained by subtracting the current density in the presence of $3\,\mu M$ SO-3 from those of Control; gray dotted line) was also plotted. Data are shown as mean$\pm$s.e.m., $n=9$ for each group. (b) I–V curves of I_{Ca} density before (Control) and after 2-min exposure to $3\,\mu M$ MVIIA ($n=7$). The $3\,\mu M$ MVIIA-sensitive current density (Control $- 3\,\mu M$ MVIIA; gray dash line) was also subtracted, and the I–V curve of $3\,\mu M$ MVIIA-sensitive current density was similar to that of $3\,\mu M$ SO-3-sensitive current density (from the same data in (a)).

physiological and pharmacological methods. Our results indicated that SO-3 had shown no effect on I_{Na}, $I_{K(DR)}$, and $I_{K(A)}$, even applied at a concentration of $100\,\mu M$ (Figures 1 and 2). However, a concentration-dependent inhibition of SO-3 on HVA I_{Ca} was observed (Figure 3), and the I–V relationship also showed the inhibitory effects of SO-3 on HVA I_{Ca} (Figure 4). We confirm that SO-3 selectively targets VSCCs, other than VSSCs or VSPCs. The ω-, κ-, μO-, and δ-conotoxins, which all belong to the O-superfamily conotoxins, target the calcium, potassium, and sodium channels, respectively (Olivera & Cruz, 2001; Terlau & Olivera, 2004). Our studies indicate that SO-3 is a new ω-conotoxin.

To date, several ω-conotoxins have been identified from fish-, worm-, or mollusk-hunting *Conus* species. Although ω-conotoxins contain the same cysteine framework as κ-, μO-, and δ-conotoxins and belong to the same O-conotoxin superfamily, they have some structural characteristics different from κ-, μO-, and δ-conotoxins. All ω-conotoxins are C-terminally post-translationally modified and amidated. Besides the conserved cysteine framework, there are three conserved residues Gly5, Tyr13, and Ser19 (numbering of MVIIA) throughout this set of peptides except SVIA (Table 1). It is known that Tyr13 residue is important for binding to the calcium channels (Kim *et al.*, 1995; Lew *et al.*, 1997; Nielsen
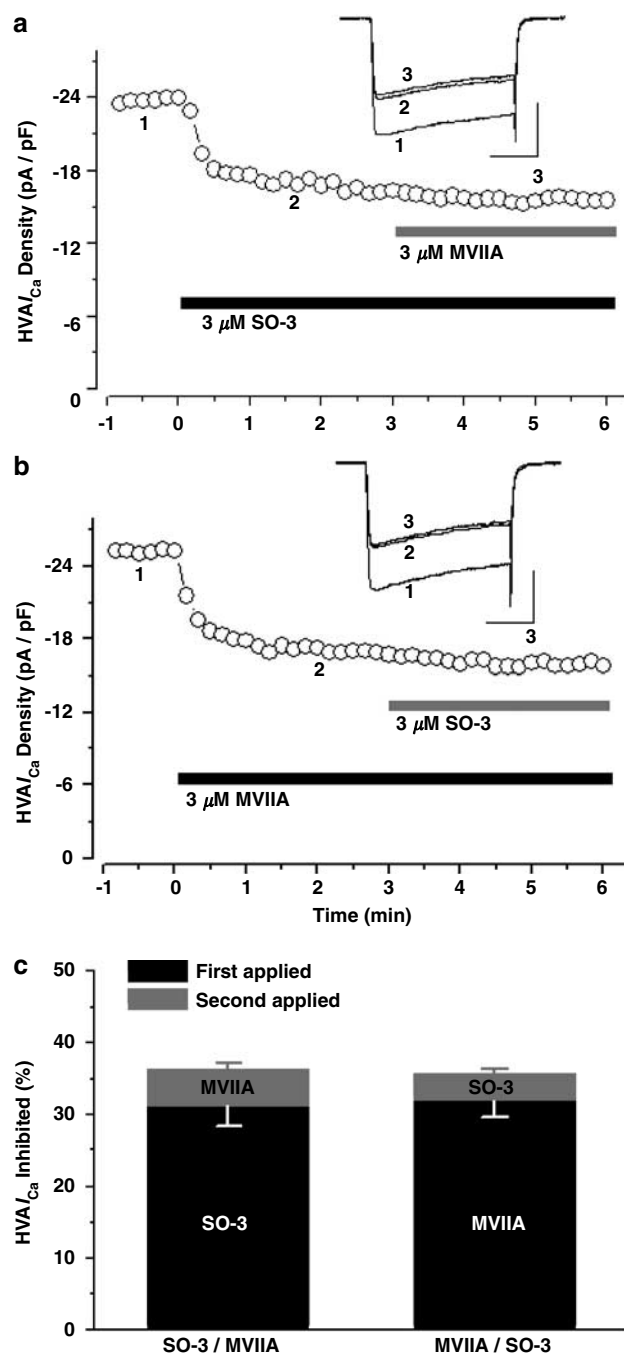
Figure 5 SO-3 and MVIIA inhibited overlapping components of the HVA I_{Ca}. (a, b) The time course showing the inhibitory effects of SO-3 (3 μM) and MVIIA (3 μM), respectively. Drugs were applied to the cell as indicated by the horizontal bars; the order of drug application was switched from SO-3 first (a) to MVIIA first (b). Currents were evoked by 150 ms depolarizing voltage step commands from −80 to 0 mV at 10 s intervals. Upper inset shows the current traces at the time points (1, 2 and 3). Scale bars: 10 pA pF^{-1}, 50 ms. The inhibition of I_{Ca} amplitude was similar whether first applied SO-3 or MVIIA, and no further inhibition was observed after additional application of another drug in each group. (c) The peak HVA I_{Ca} inhibited by SO-3 and MVIIA were converted to a fraction of the total currents. Data are shown as mean ± s.e.m., for both SO-3 applied first and MVIIA applied first, $n = 8$. Two-way ANOVA on repeated measures (RM), $P = 0.872$ for drug type, $P < 0.001$ for presentation order, $P = 0.478$ for interaction.
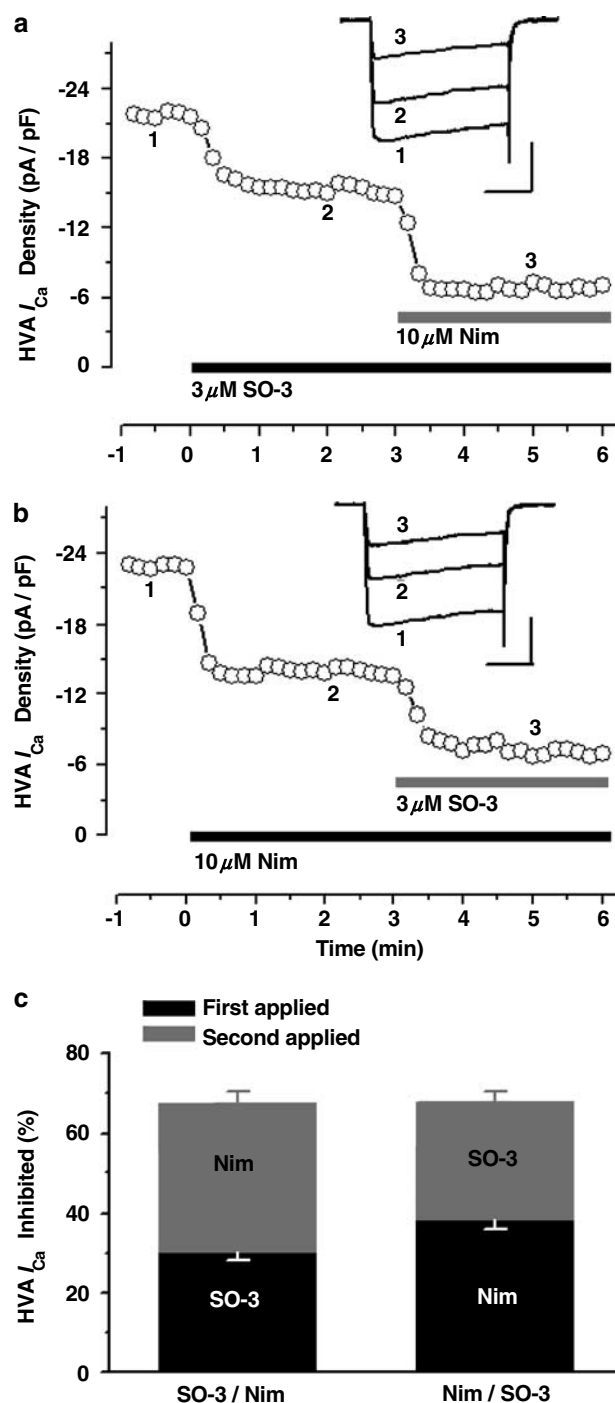
Figure 6 SO-3 and nimodipine (Nim) inhibited nonoverlapping components of HVA I_{Ca}. (a, b) shows the time course of the inhibitory effects of SO-3 (3 μM) and Nim (10 μM) on peak HVA I_{Ca}, with switching the order of drug application from SO-3 first (a) to Nim first (b). The elicited current protocol was the same as that in Figure 5. The upper inset shows the example recordings made at the time points 1, 2, and 3. Scale bars: 10 pA pF^{-1}, 50 ms. (c) shows that the calculated fraction of HVA I_{Ca} inhibited by SO-3 and Nim was unchanged by switching the order of drug application from SO-3 first to Nim first, the percentage inhibition of Nim (∼38%) was greater than that of SO-3 (∼30%). Data are shown as mean ± s.e.m., for both SO-3 applied first and Nim applied first, $n = 8$. Two-way ANOVA on RM, $P = 0.008$ for drug type, $P = 0.682$ for presentation order, $P = 0.974$ for interaction.

a

0.5 μM Aga

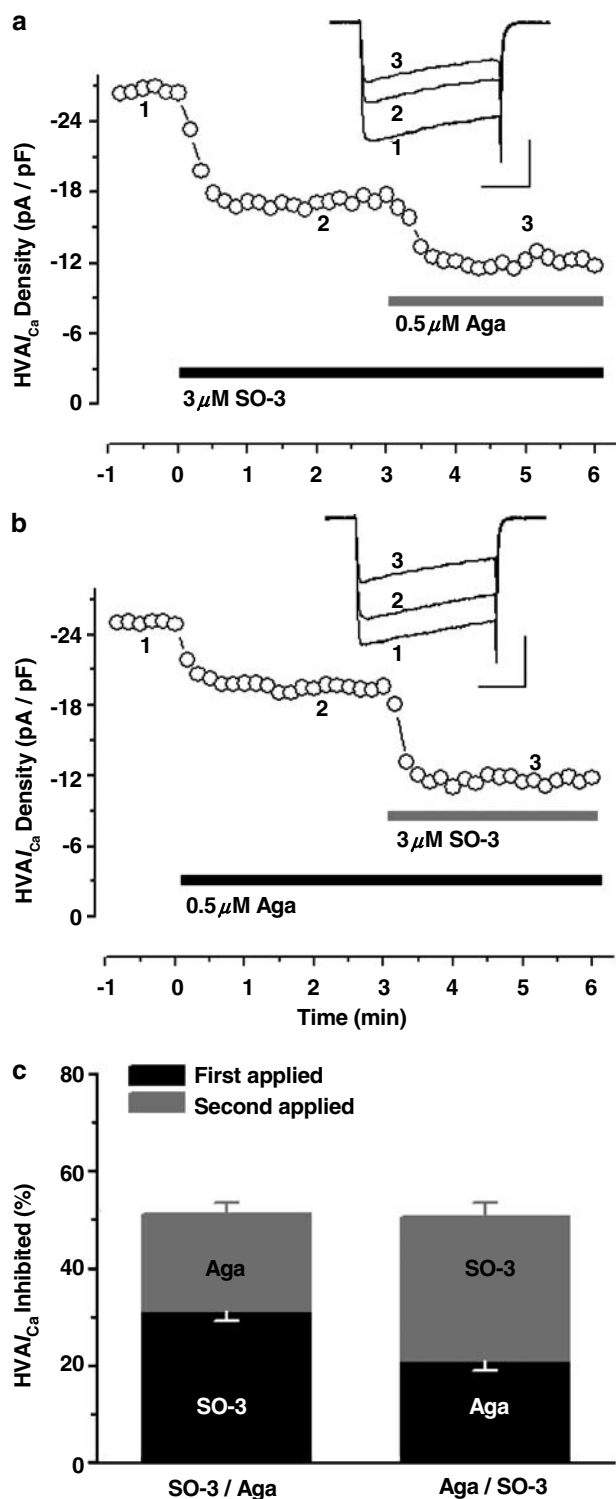3 μM SO-3

b

3 μM SO-3

0.5 μM Aga

c

Figure 7 SO-3 and ω-agatoxin (Aga) inhibited nonoverlapping components of HVA I_{Ca}. The time course (a, b) and the histograms (c) show that the fraction of HVA I_{Ca} inhibited by SO-3 (3 μM) and Aga (0.5 μM) was unchanged by switching the order of drug application from SO-3 first to Aga first; the percentage inhibition of SO-3 ($\sim$31%) was greater than that of Aga ($\sim$21%). The experiment protocol was as same as that in Figure 5 and 6. Two-way ANOVA on RM, $P = 0.001$ for drug type, $P = 0.544$ for presentation order, $P = 0.923$ for interaction. Data are shown as mean ± s.e.m., for both SO-3 applied first and Aga applied first, $n = 7$. Scale bars: 10 pA pF^{-1}, 50 ms.
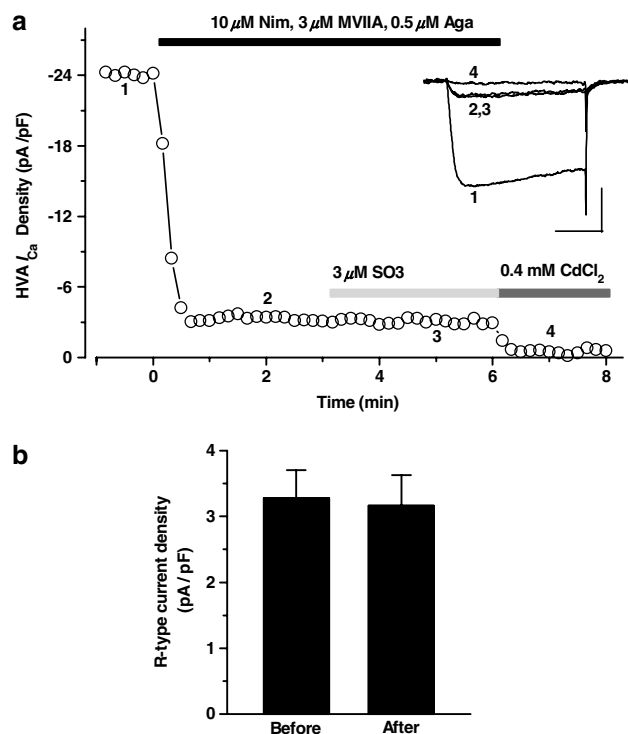
a

b

Figure 8 No effect of SO-3 on R-type HVA I_{Ca}. (a) R-type currents were isolated after application of 10 μM Nim, 3 μM MVIIA and 0.5 μM Aga and contributed $\sim$12% of the total HVA I_{Ca}. After additional application of 3 μM SO-3, no obvious R-type current was further inhibited, but these currents were almost completely blocked by 0.4 mM CdCl$_2$. The inset shows the current traces at each time points. Currents were evoked by 150 ms depolarizing voltage step commands from −80 to 0 mV at 10 s intervals. Scale bars: 10 pA pF^{-1}, 50 ms. (b) The histograms for R-type current density before and after application of 3 μM SO-3 (paired Student's *t*-test, $P > 0.05$). Data are shown as mean ± s.e.m., $n = 7$.

et al., 1999b). Apart from these characteristics, all ω-conotoxins possess 4–6 positive charges due to the high content of basic amino-acid residues, which are also known to play an important role in the blocking of calcium channels (Lew *et al.*, 1997; Nielsen *et al.*, 2000). Among these three conotoxins derived from *C. striatus*, SVIA is the smallest ω-conotoxin without the Tyr13, Ser19 residues, and has relatively poor activity on most calcium channels found in mammalian systems (Ramilo *et al.*, 1992), whereas SO-3 has primary structural characteristics similar to SVIB and other derived ω-conotoxins, which may contribute to its selectivity on VSCCs.

VSCCs subtype selectivity of SO-3

As reported before, MVIIA (3 μM), nimodipine (10 μM) and Aga (0.5 μM) can selectively block the N-, L-, and P/Q-type I_{Ca} in hippocampal neurons, respectively (Currie & Fox, 1997; Nakashima *et al.*, 1998; Blalock *et al.*, 1999; Scamps *et al.*, 2000). In the present studies, 3 μM MVIIA-, 10 μM nimodipine-, 0.5 μM Aga-sensitive currents in cultured hippocampal neurons contributed $\sim$32, $\sim$38, and $\sim$21% of HVA I_{Ca}, respectively, which were consistent with the previous studies (Nakashima *et al.*, 1998; Blalock *et al.*, 1999; Scamps *et al.*, 2000). SO-3 (3 μM)-sensitive currents contributed $\sim$31% of HVA I_{Ca}, which was very similar to the percentage of MVIIA-sensitive
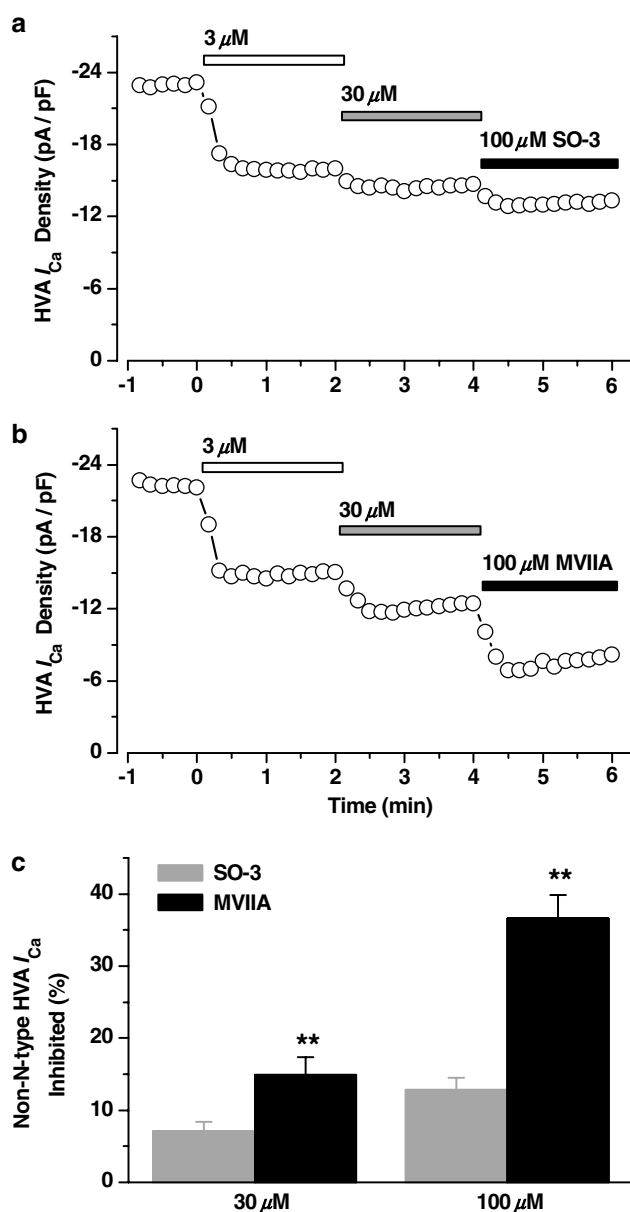
Figure 9 Higher concentrations of SO-3 and MVIIA inhibited non-N-type HVA I_{Ca} in cultured hippocampal neurons. (a, b) The time course showing the inhibitory effects of 3, 30, and 100 μM SO-3 (a) and MVIIA (b) on peak HVA I_{Ca}, respectively. Currents were evoked by 150 ms depolarizing voltage step commands from -80 to 0 mV at 10 s intervals. (c) The non-N-type HVA I_{Ca} inhibited by 30 and 100 μM SO-3 and MVIIA were converted to a fraction of the total currents. Data are shown as mean$\pm$s.e.m. For SO-3 groups, $n = 8$, and for MVIIA, $n = 6$. **$P < 0.01$; statistically significant difference from the effect of the same concentration of SO-3 (unpaired Student's *t*-test).

currents. SO-3 and MVIIA inhibited the overlapping components of HVA I_{Ca} in cultured hippocampal neurons, and no overlapping component of HVA I_{Ca} was inhibited by SO-3 and nimodipine, or by SO-3 and Aga (Figures 5–7). These results suggest that SO-3 shares a common site of inhibition with MVIIA, but not with nimodipine and Aga. Our research also demonstrated that 3 μM SO-3 had no effect on R-type HVA I_{Ca} (Figure 8). These results indicate that SO-3 selectively blocks N-type VSCCs and does not inhibit L-, P/Q- and R-type currents at this concentration.
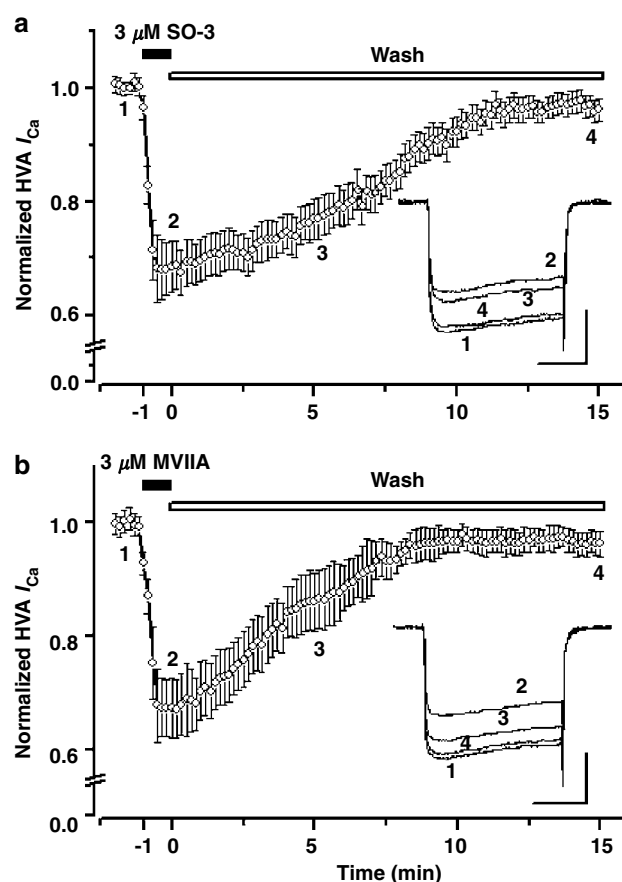

Figure 10 Reversibility of the inhibitory effects of SO-3 on HVA I_{Ca}. Currents were evoked by 150 ms depolarizing voltage step commands from -80 to 0 mV at 10 s intervals and were normalized to the values before application of 3 μM SO-3 (upper) and 3 μM MVIIA (lower). Both SO-3 and MVIIA were applied to the cells for 60 s. The inhibitory effects of SO-3 and MVIIA on HVA I_{Ca} were almost completely reversed after washing $\sim$12 min (SO-3) and $\sim$10 min (MVIIA), and the recovery from block by MVIIA was more rapid than recovery from block by SO-3. Data are shown as mean$\pm$s.e.m., both $n = 7$. The inset shows the sample current traces at each time points. Scale bars: 10 pA pF^{-1}, 50 ms.

Both ω-conotoxins SVIB and SO-3 were isolated from *C. striatus*. SVIB is selective for the P/Q-type VSCCs (Ramilo *et al.*, 1992), whereas SO-3 is shown to selectively target the N-type VSCCs in the present study. SO-3 demonstrates a 56% sequence identity to SVIB and a higher (72%) sequence identity to MVIIA. However, the identity in primary sequences is insufficient to define VSCC selectivity. Sequence hypervariability has been observed between functionally homologous ω-conotoxins. ω-Conotoxins with high sequence identity may also demonstrate different selectivities (Table 1). Therefore, studies of secondary and tertiary structures of SO-3 and other ω-conotoxins might help much to understand the subtype selectivity in blocking VSCCs. The three-dimensional solution structure of SO-3 was determined by ^{1}H NMR and showed that it contains a short antiparallel β-sheet involving residues 6–9, 19–21, and 24–25 similar to MVIIA, and the disulfide bridge pattern of SO-3 was also identical to the cystine framework that found in MVIIA and other ω-conotoxins (Yan *et al.*, 2003). These results indicate that the identity of SO-3 and MVIIA in three-dimensional structure contribute to their selectively targeting the same N-type VSCCs. Additionally, the

previous structure–activity analysis of ω-conotoxins also indicates that loops 1 and 3 have little effect on selectivity, whereas loops 2 and 4 are critical determinants in controlling the selectivity of ω-conotoxins for N- or P/Q-, R-type VSCCs (Nielsen *et al.*, 1999a; 2000; Lewis *et al.*, 2000). Hence, the assumption that SO-3 and SVIB target different VSCC subtypes due to the difference in their three-dimensional structure requires further studies.

Reversibility of the inhibitory effects of SO-3 on HVA I_{Ca}

Previously, some researchers have reported and discussed the reversibility of the blocking effects of several ω-conotoxins on the transiently expressed N-type VSCCs and these results are not consistent with each other. Taken together, the blocking effect of GVIA is poorly reversible, while that of both MVIIA and CVID are readily reversible (Williams *et al.*, 1992a; Kristipati *et al.*, 1994; Lin *et al.*, 1997; Stocker *et al.*, 1997; Feng *et al.*, 2001; 2003; Liang & Elmslie, 2002; Mould *et al.*, 2004). Since ω-conotoxin GVIA dissociates very slowly from VSCCs, it may be difficult to control in a clinical setting, and is therefore not an ideal drug candidate. In our study, the inhibitory effects of SO-3 and MVIIA on HVA I_{Ca} in primary cultured hippocampal neurons were both almost completely reversed, and the recovery from block by MVIIA was more rapid than recovery from block by SO-3 (Figure 10). The recovery from block by ω-conotoxins is partly dependent on the divalent cations in extracellular solution (Liang & Elmslie, 2002), the V_{h} (Stocker *et al.*, 1997; Feng *et al.*, 2003), and the $\alpha_2\delta$ auxiliary subunit of VSCCs (Mould *et al.*, 2004). Apart from these, the amino-acid residue of ω-conotoxins at position 10 has a significant impact on the extent of the reversibility of these toxins (Mould *et al.*, 2004). SO-3 and MVIIA, both with Arg at position 10 (Table 1), can reversibly block the VSCCs, whereas GVIA demonstrates different reversibility because of the different residue (Hyp) at position 10 (Table 1). The different extent of recovery from the block by SO-3 and MVIIA may due to the different sequence of the amino-acid residues near this position or other unknown mechanisms.

Potential therapeutic implications

N-type calcium channels located in pre-synaptic nerve terminals regulate the influx of calcium which is necessary for neurotransmitter release in both the central and peripheral nervous systems (Jarvis & Zamponi, 2001; Zamponi, 2003). Selective blockers of N-type VSCCs may have potential neuroprotective application in ischemic brain injury by increasing blood flow, reducing glutamate release, and reducing postsynaptic calcium influx (Pringle *et al.*, 1996; Bowersox *et al.*, 1997). However, considerable research in the last decade has focused on the therapeutic potential of the

N-type VSCCs blockers as a new class of analgesic agents (Vanegasa & Schaible, 2000; Scott *et al.*, 2002). N-type calcium channels are highly present at the pre-synaptic terminals of nociceptive neurons in dorsal horn of the spinal cord where they regulate the release of the key pro-nociceptive neurotransmitters such as glutamate, substance P, neurokinin A, and/or calcitonin gene-related peptide (Jarvis & Zamponi, 2001; Adams *et al.*, 2003). The crucial role of the N-type channels in nociception is also supported by the evidence that mice lacking the N-type channel gene have higher pain thresholds compared to wild type (Hatakeyama *et al.*, 2001; Kim *et al.*, 2001; Saegusa *et al.*, 2002).

Recently, the pain-relieving effects of several ω-conotoxins have been characterized. MVIIA (also known as SNX-111, Ziconotide or Prialt) is under phase III clinical trial in humans with severe intractable pain (Staats *et al.*, 2004; Doggrell, 2004). Another peptide, CVID (also known as AM336), is more selective towards the N-type VSCC than MVIIA, may have superior clinical utility and lower side-effects relative to MVIIA for the alleviation of persistent pain states (Scott *et al.*, 2002; Smith *et al.*, 2002). Our previous studies also showed that SO-3 displays an analgesic potency similar to MVIIA in a range of acute and chronic pain models in rodents, yet has less adverse effects compared with identical dosages of MVIIA injected intrathecally (Dai *et al.*, 2003).

The neurotransmitter release from most central synapses is mainly controlled by P/Q- and R-type calcium channels (Meir *et al.*, 1999), and, P/Q-type VSCCs exists primarily in neuromuscular junction, selective P/Q-type VSCCs blockers (such as MVIIC and SVIB) are likely to be lethal at relatively low dose and are considered unuseful in pain treatment (Bowersox *et al.*, 1995; Katz *et al.*, 1997). Consequently, ω-conotoxin more selective for N-type VSCCs than P/Q and other type VSCCs can largely minimize the side-effects in analgesic therapy. As mentioned previously, SO-3 does not inhibit L-, P/Q-, and R-type currents at the concentrations $(1-3\,\mu\mathrm{M})$ where its inhibition on N-type currents is maximum (Figures 5–8), and it has less effects on non-N-type HVA currents than MVIIA at higher concentrations (30 and $100\,\mu\mathrm{M}$) (Figure 9), which may contribute to the different side-effects of SO-3 and MVIIA observed in previous animal experiments. These characteristics also indicate that SO-3 may have more advantages in clinical field as an analgesic candidate.

References

ADAMS, D.J., SMITH, A.B., SCHROEDER, C.I., YASUDA, T. & LEWIS, R.J. (2003). ω-Conotoxin CVID inhibits a pharmacologically distinct voltage-sensitive calcium channel associated with transmitter release from preganglionic nerve terminals. *J. Biol. Chem.*, **278**, 4057–4062.

BANKER, G.A. & COWAN, W.M. (1979). Further observations on hippocampal neurons in dispersed cell culture. *J. Comp. Neurol.*, **187**, 469–493.

BLALOCK, E.M., PORTER, N.M. & LANDFIELD, P.W. (1999). Decreased G-protein-mediated regulation and shift in calcium channel types with age in hippocampal cultures. *J. Neurosci.*, **19**, 8674–8684.

BOWERSOX, S.S., MILJANICH, G.P., SUGIURA, Y., LI, C., NADASDI, L., HOFFMAN, B.B., RAMACHANDRAN, J. & KO, C.P. (1995). Differential blockade of voltage-sensitive calcium channels at the mouse neuromuscular junction by novel ω-conopeptides and ω-agatoxin-IVA. *J. Pharmacol. Exp. Ther.*, **273**, 248–256.

BOWERSOX, S.S., SINGH, T. & LUTHER, R.R. (1997). Selective blockade of N-type voltage-sensitive calcium channels protects against brain injury after transient focal cerebral ischemia in rats. *Brain Res.*, **747**, 343–347.

BULAJ, G., DELACRUZ, R., AZIMI-ZONOOZ, A., WEST, P., WATKINS, M., YOSHIKAMI, D. & OLIVERA, B.M. (2001). Conotoxin structure/function through a cladistic analysis. *Biochemistry*, **40**, 13201–13208.

CURRIE, K.P.M. & FOX, A.P. (1997). Comparison of N- and P/Q-type voltage-gated calcium channel current inhibition. *J. Neurosci.*, **17**, 4570–4579.

DAI, Q., LIU, F., ZHOU, Y., LU, B., YU, F. & HUANG, P. (2003). The synthesis of SO-3, a conopeptide with high analgesic activity derived from *Conus striatus*. *J. Nat. Prod.*, **66**, 1276–1279.

DOGGRELL, S.A. (2004). Intrathecal ziconotide for refractory pain. *Expert Opin. Investig. Drugs*, **13**, 875–877.

FENG, Z.P., DOERING, C.J., WINKFEIN, R.J., BEEDLE, A.M., SPAFFORD, J.D. & ZAMPONI, G.W. (2003). Determinants of inhibition of transiently expressed voltage-gated calcium channels by ω-conotoxins GVIA and MVIIA. *J. Biol. Chem.*, **278**, 20171–20178.

FENG, Z.P., HAMID, J., DOERING, C., BOSEY, G.M., SNUTCH, T.P. & ZAMPONI, G.W. (2001). Residue Gly^{1326} of the N-type calcium channel α_{1B} subunit controls reversibility of ω-conotoxin GVIA and MVIIA block. *J. Biol. Chem.*, **276**, 15728–15735.

HAMILL, O.P., MARTY, A., NEHER, E., SAKMANN, B. & SIGWORTH, F.J. (1981). Improved patch-clamp techniques for high-resolution current recording from cells and cell-free membrane patches. *Pflügers Arch.*, **391**, 85–100.

HATAKEYAMA, S., WAKAMORI, M., INO, M., MIYAMOTO, N., TAKAHASHI, E., YOSHINAGA, T., SAWADA, K., IMOTO, K., TANAKA, I., YOSHIZAWA, T., NISHIZAWA, Y., MORI, Y., NIIDOME, T. & SHOJI, S. (2001). Differential nociceptive responses in mice lacking the α_{1B} subunit of N-type Ca^{2+} channels. *Neuroreport*, **12**, 2423–2427.

HILLYARD, D.R., MONJE, V.D., MINTZ, I.M., BEAN, B.P., NADASDI, L., RAMACHANDRAN, J., MILJANICH, G., AZIMI-ZOONOOZ, A., MCINTOSH, J.M., CRUZ, L.J., IMPERIAL, J.S. & OLIVERA, B.M. (1992). A new *Conus* peptide ligand for mammalian presynaptic Ca^{2+} channels. *Neuron*, **9**, 69–77.

JARVIS, E.S. & ZAMPONI, G.W. (2001). Interactions between presynaptic Ca^{2+} channels, cytoplasmic messengers and proteins of the synaptic vesicle release complex. *Trends Pharmacol. Sci.*, **22**, 519–525.

KATZ, E., PROTTI, D.A., FERRO, P.A., ROSATO, S. & UCHITEL, O.D. (1997). Effects of Ca^{2+} channel blocker neurotoxins on transmitter release and presynaptic currents at the mouse neuromuscular junction. *Br. J. Pharmacol.*, **121**, 1531–1540.

KIM, C., JUN, K., LEE, T., KIM, S.S., MCENERY, M.W., CHIN, H., KIM, H.L., PARK, J.M., KIM, D.K., JUNG, S.J., KIM, J. & SHIN, H.S. (2001). Altered nociceptive response in mice deficient in the α_{1B} subunit of the voltage-dependent calcium channel. *Mol. Cell Neurosci.*, **18**, 235–245.

KIM, J.I., TAKAHASHI, M., OHTAKE, A., WAKAMIYA, A. & SATO, K. (1995). Tyr13 is essential for the activity of ω-conotoxin mviia and gvia, specific N-type calcium channel blockers. *Biochem. Biophys. Res. Commun.*, **206**, 449–454.

KRISTIPATI, R., NADASDI, L., TARCZY-HORNOCH, K., LAU, K., MILJANICH, G.P., RAMACHANDRAN, J. & BELL, J.R. (1994). Characterization of the binding of ω-Conopeptides to different classes of non-L-type neuronal calcium channels. *Mol. Cell Neurosci.*, **5**, 219–228.

LEW, M.J., FLINN, J.P., PALLAGHY, P.K., MURPHY, R., WHORLOW, S.L., WRIGHT, C.E., NORTON, R.S. & ANGUS, J.A. (1997). Structure–function relationships of ω-conotoxin GVIA. Synthesis, structure, calcium channel binding, and functional assay of alanine-substituted analogs. *J. Biol. Chem.*, **272**, 12014–12023.

LEWIS, R.J., NIELSEN, K.J., CRAIK, D.J., LOUGHNAN, M.L., ADAMS, D.A., SHARPE, I.A., LUCHIAN, T., ADAMS, D.J., BOND, T., THOMAS, L., JONES, A., MATHESON, J.L., DRINKWATER, R., ANDREWS, P.R. & ALEWOOD, P.F. (2000). Novel ω-conotoxins from *Conus catus* discriminate among neuronal calcium channel subtypes. *J. Biol. Chem.*, **275**, 35335–35344.

LIANG, H. & ELMSLIE, K.S. (2002). Rapid and reversible block of N-type calcium channels (Ca_V 2.2) by ω-conotoxin GVIA in the absence of divalent cations. *J. Neurosci.*, **22**, 8884–8890.

LIN, Z., HAUS, S., EDGERTON, J. & LIPSCOMBE, D. (1997). Identification of functionally distinct isoforms of the N-type Ca^{2+} channel in rat sympathetic ganglia and brain. *Neuron*, **18**, 153–166.

LU, B.S., YU, F., ZHAO, D., HUANG, P.T. & HUANG, C.F. (1999). Conopeptides from *Conus striatus* and *Conus textile* by cDNA cloning. *Peptides*, **20**, 1139–1144.

MCINTOSH, J.M., HASSON, A., SPIRA, M.E., GRAY, W.R., LI, W., MARSH, M., HILLYARD, D.R. & OLIVERA, B.M. (1995). A new family of conotoxins that blocks voltage-gated sodium channels. *J. Biol. Chem.*, **270**, 16796–16802.

MEIR, A., GINSBURG, S., BUTKEVICH, A., KACHALSKY, S.G., KAISERMAN, I., AHDUT, R., DEMIRGOREN, S. & RAHAMIMOFF, R. (1999). Ion channels in presynaptic nerve terminals and control of transmitter release. *Physiol. Rev.*, **79**, 1019–1088.

MOULD, J., YASUDA, T., SCHROEDER, C.I., BEEDLE, A.M., DOERING, C.J., ZAMPONI, G.W., ADAMS, D.J. & LEWIS, R.J. (2004). The $\alpha_2\delta$ auxiliary subunit reduces affinity of ω-conotoxins for recombinant N-type ($Ca_v2.2$) calcium channels. *J. Biol. Chem.*, **279**, 34705–34714.

NAKASHIMA, Y.M., TODOROVIC, S.M., COVEY, D.F. & LINGLE, C.J. (1998). The anesthetic steroid (+)-3α-hydroxy-5α-androstane-17β-carbonitrile blocks N-, Q-, and R-type, but not L- and P-type, high voltage-activated Ca^{2+} current in hippocampal and dorsal root ganglion neurons of the rat. *Mol. Pharmacol.*, **54**, 559–568.

NEWCOMB, R., SZOKE, B., PALMA, A., WANG, G., CHEN, X.H., HOPKINS, W., CONG, R., MILLER, J., URGE, L., TARCZY-HORNOCH, K., LOO, J.A., DOOLEY, D.J., NADASDI, L., TSIEN, R.W., LEMOS, J. & MILJANICH, G. (1998). Selective peptide antagonist of the class E calcium channel from the venom of the tarantula *Hysterocrates gigas*. *Biochemistry*, **37**, 15353–15362.

NIELSEN, K.J., ADAMS, D., THOMAS, L., BOND, T., ALEWOOD, P.F., CRAIK, D.J. & LEWIS, R.J. (1999a). Structure–activity relationships of ω-conotoxins MVIIA, MVIIC and 1, 4 loop splice hybrids at N and P/Q-type calcium channels. *J. Mol. Biol.*, **289**, 1405–1421.

NIELSEN, K.J., ADAMS, D.A., ALEWOOD, P.F., LEWIS, R.J., THOMAS, L., SCHROEDER, T. & CRAIK, D.J. (1999b). Effects of chirality at Tyr^{13} on the structure–activity relationships of ω-conotoxins from *conus magus*. *Biochemistry*, **38**, 6741–6751.

NIELSEN, K.J., SCHROEDER, T. & LEWIS, R. (2000). Structure–activity relationships of ω-conotoxins at N-type voltage-sensitive calcium channels. *J. Mol. Recognit.*, **13**, 55–70.

OLIVERA, B.M. & CRUZ, L.J. (2001). Conotoxins, in retrospect. *Toxicon*, **39**, 7–14.

OLIVERA, B.M., MCINTOSH, J.M., CRUZ, L.J., LUQUE, F.A. & GRAY, W.R. (1984). Purification and sequence of a presynaptic peptide toxin from *Conus geographus* venom. *Biochemistry*, **23**, 5087–5090.

PRINGLE, A.K., BENHAM, C.D., SIM, L., KENNED, Y.J., IANNOTTI, F. & SUNDSTROM, L.E. (1996). Selective N-type calcium channel antagonist omega conotoxin MVIIA is neuroprotective against hypoxic neurodegeneration in organotypic hippocampal-slice cultures. *Stroke*, **27**, 2124–2130.

RAMILO, C.A., ZAFARALLA, G.C., NADASDI, L., HAMMERLAND, L.G., YOSHIKAMI, D., GRAY, W.R., KRISTIPATI, R., RAMACHANDRAN, J., MILJANICH, G. & OLIVERA, B.M. (1992). Novel α- and ω-conotoxins from *Conus striatus* venom. *Biochemistry*, **31**, 9919–9926.

SAEGUSA, H., MATSUDA, Y. & TANABE, T. (2002). Effects of ablation of N- and R-type Ca^{2+} channels on pain transmission. *Neurosci. Res.*, **43**, 1–7.

SCAMPS, F., VIGUES, S., RESTITUITO, S., CAMPO, B., ROIG, A., CHARNET, P. & VALMIER, J. (2000). Sarco-endoplasmic ATPase blocker 2, 5-di (*tert*-butyl)-1, 4-benzohydroquinone inhibits N-, P-, and Q- but not T-, L-, or R-type calcium currents in central and peripheral neurons. *Mol. Pharmacol.*, **58**, 18–26.

SCOTT, D.A., WRIGHT, C.E. & ANGUS, J.A. (2002). Actions of intrathecal ω-conotoxins CVID, GVIA, MVIIA, and morphine in acute and neuropathic pain in the rat. *Eur. J. Pharmacol.*, **451**, 279–286.

SHON, K., STOCKER, M., TERLAU, H., STUHMER, W., JACOBSEN, R., WALKER, C., GRILLEY, M., WATKINS, M., HILLYARD, D.R., GRAY, W.R. & OLIVERA, B.M. (1998). Conotoxin PVIIA: a peptide inhibiting the shaker K^+ channel. *J. Biol. Chem.*, **273**, 33–38.

SMITH, M.T., CABOT, P.J., ROSS, F.B., ROBERTSON, A.D. & LEWIS, R.J. (2002). The novel N-type calcium channel blocker, AM336, produces potent dose-dependent antinociception after intrathecal dosing in rats and inhibits substance P release in rat spinal cord slices. *Pain*, **96**, 119–127.

STAATS, P.S., YEARWOOD, T., CHARAPATA, S.G., PRESLEY, R.W., WALLACE, M.S., BYAS-SMITH, M., FISHER, R., BRYCE, D.A., MANGIERI, E.A., LUTHER, R.R., MAYO, M., MCGUIRE, D. & ELLIS, D. (2004). Intrathecal ziconotide in the treatment of refractory pain in patients with cancer or AIDS: a randomized controlled trial. *JAMA*, **291**, 63–70.

STOCKER, J.W., NADASDI, L., ALDRICH, R.W. & TSIEN, R.W. (1997). Preferential interaction of ω-conotoxins with inactivated N-type ca^{2+} channels. *J. Neurosci.*, **17**, 3002–3013.

TERLAU, H. & OLIVERA, B.M. (2004). *Conus* venoms: a rich source of novel ion channel-targeted peptides. *Physiol. Rev.*, **84**, 41–68.

VANEGASA, H. & SCHAIBLE, H.G. (2000). Effects of antagonists to high-threshold calcium channels upon spinal mechanisms of pain, hyperalgesia and allodynia. *Pain*, **8**, 9–18.

WILLIAMS, M.E., BRUST, P.F., FELDMAN, D.H., PATTHI, S., SIMERSON, S., MAROUFI, A., MCCUE, A.F., VELICELEBI, G., ELLIS, S.B. & HARPOLD, M.M. (1992a). Structure and functional expression of an ω-conotoxin-sensitive human N-type calcium channel. *Science*, **257**, 389–395.

WILLIAMS, M.E., FELDMAN, D.H., MCCUE, A.F., BRENNER, R., VELICELEBI, G., ELLIS, S.B. & HARPOLD, M.M. (1992b). Structure and functional expression of $\alpha 1$, $\alpha 2$, and β subunits of a novel human neuronal calcium channel subtype. *Neuron*, **8**, 71–84.

YAN, Y.B., TU, G.Z., LUO, X.C., DAI, Q.Y., HUANG, P.T. & ZHANG, R.Q. (2003). Three-dimensional solution structure of ω-conotoxin SO3 determined by ^{1}HNMR. *Chin. Sci. Bull.*, **48**, 1097–1102.

YANG, F., FENG, L., ZHENG, F., JOHNSON, S.W., DU, J., SHEN, L., WU, C.P. & LU, B. (2001). GDNF acutely modulates excitability and A-type K$^+$ channels in midbrain dopaminergic neurons. *Nat. Neurosci.*, **4**, 1071–1078.

ZAMPONI, G.W. (2003). Regulation of presynaptic calcium channels by synaptic proteins. *J. Pharmacol. Sci.*, **92**, 79–83.

ZHANG, J.F., RANDALL, A.D., ELLINOR, P.T., HORNE, W.A., SATHER, W.A., TANABE, T., SCHWARZ, T.L. & TSIEN, R.W. (1993). Distinctive pharmacology and kinetics of cloned neuronal Ca^{2+} channels and their possible counterparts in mammalian CNS neurons. *Neuropharmacology*, **32**, 1075–1088.